



Project report

## **Internal Perforated-steel-plate Connections with Self-Drilling Dowels for Cross-laminated Timber**

November 05, 2020

Prepared by

**Maximilian Drexler**

MEng Student  
Department of Civil Engineering  
University of Applied Sciences Munich  
[max-drexler@gmx.net](mailto:max-drexler@gmx.net)

and

**Thomas Tannert, PhD, PEng**

Professor, School of Engineering  
Canada Research Chair, BC Leadership Chair  
University of Northern British Columbia  
<http://blogs.unbc.ca/thomastannert>  
[thomas.tannert@unbc.ca](mailto:thomas.tannert@unbc.ca)  
Tel: 250-960-6710

## **Executive Summary**

Cross-laminated timber (CLT) constitutes a promising solution for numerous structural applications, including for large and tall residential and commercial buildings. The prospect of building larger timber structures creates some structural challenges, amongst them being that lateral forces created by high winds and strong earthquakes are higher and create higher demands of “hold-downs”. The Canadian Standard for Engineering Design in Wood CSA-O86 does not (yet) provide any specific procedures to estimate the resistance of mass-timber Lateral Load Resisting Systems (LLRS) nor how to facilitate the targeted kinematic mode, especially for multi-panel walls where the LLRS behaviour is a function of connection behaviour.

The project investigated the viability of internal-perforated-steel-plates (ISP) with self-drilling dowels as high-performance connections for CLT LLRS. The project objective was to contribute towards the development of reliable design guidance for ISP connections. To achieve this objective, first at the material level, the properties of the used steel-plates and dowels were verified. Then, at the component level, the performance of shear connections and hold-downs were investigated by performing quasi-static monotonic and reversed cyclic tests.

The most significant finding of the component level tests was the proof that it is possible to control the strength, stiffness, and ductility only through the IPSP and avoid bending of the SDD or crushing of the wood. Furthermore, the length of the steel perforations had a large impact on the performance with the steel-plates with the long slots (Type-D and Type-E) exhibiting lower strength and stiffness. For the hold-down tests, the same perforation geometry as for the shear-connection tests was chosen. As already determined in the shear-connection tests, the hold-down specimens with the short perforation slots resulted in the strongest and stiffest connection.

The results from this project will be used to design and test CLT shear walls with ISP connections.

## Table of Contents

1. Test Overview .....	1
2. Materials .....	2
3. Material Level Tests.....	3
3.1 Dowel Bending Tests	3
3.2 Tension Tests of Neck-Shaped Steel-Plates	5
3.3 Shear-Tension Tests of Perforated Steel-Plates	5
4. Shear-Connection Tests.....	7
4.1 Overview	7
4.2 Specimen Geometry	7
4.3 Methods	9
5. Hold-Down Tests .....	10
5.1 Specimen Geometry	10
5.2 Methods	11
6. Analysis.....	12
7. Results .....	14
7.1 Dowel Bending Tests	14
7.2 Steel-Plate Tests	15
7.3 CLT Shear-Connection Tests	17
7.4 Hold-Down Tests	23
References.....	26
Acknowledgments .....	27

## 1. Test Overview

The main objective of this thesis was to investigate the viability of internal-perforated steel-plates (IPSP) with self-drilling dowels (SDD) as high-performance connections for cross-laminated timber (CLT) lateral load resisting systems (LLRS). Experimental investigations on the material and component levels for connections with perforated steel-plates and self-drilling dowels were conducted. The flowchart in Figure 1 gives an overview of the conducted investigations.

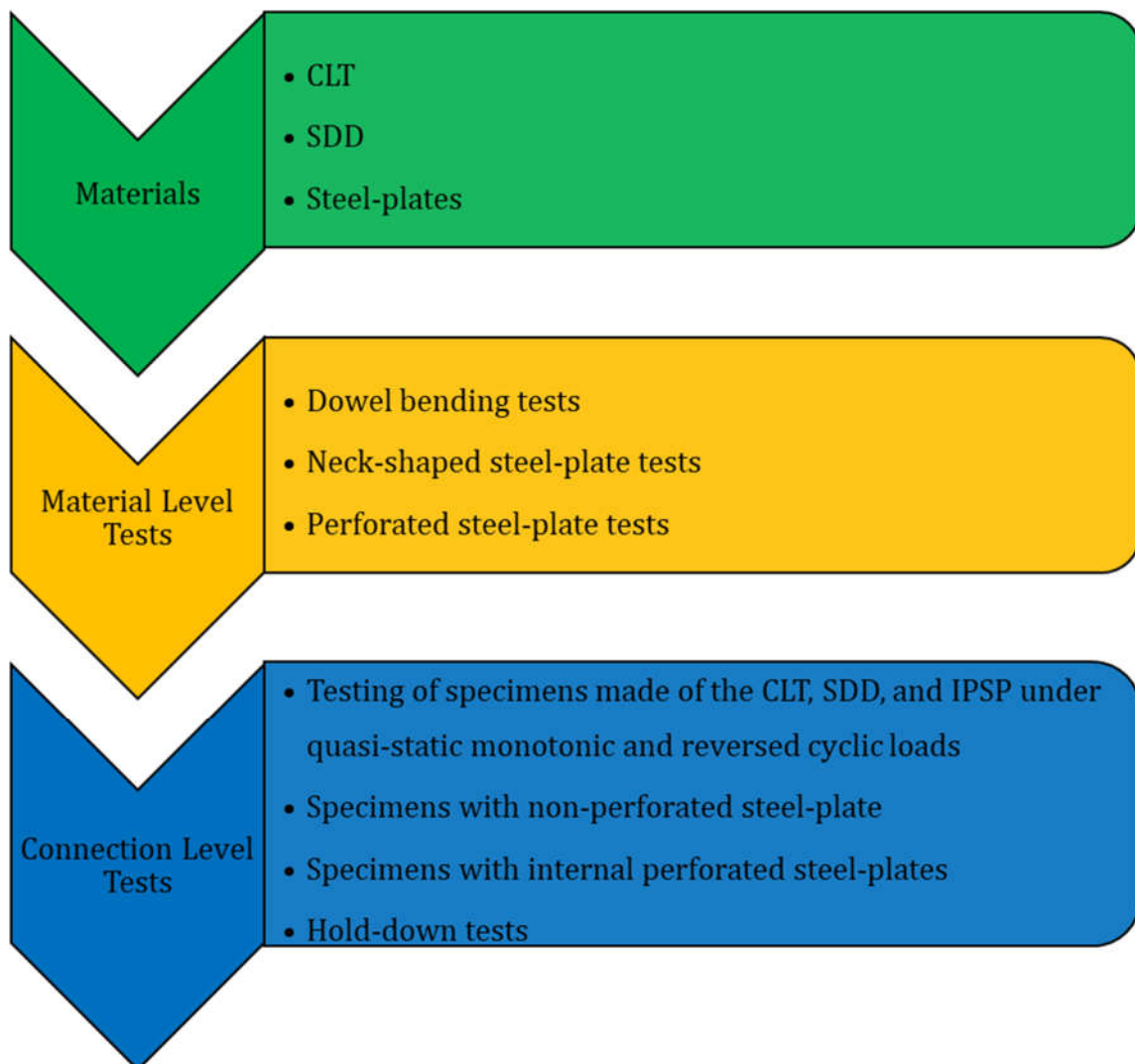


Figure 1: Flowchart for experimental investigations

The first step of the project was to start at the material level and investigate the behaviour, the performance, and the properties of the SDD and the used steel-plates. To verify the characterizing values of the SDD, dowel bending tests were performed. To investigate the used steel, tension tests with neck-shaped steel-plates were carried out. These initial experiments and investigations form the basis for the further procedure.

The second step consisted of the testing of the IPSP under shear and tension. These shear-tension tests investigated the important parameters like the impact of the perforation size, the shape, and spacing on strength, stiffness, and ductility. This step provided insight into the required parameter combinations to facilitate the desired steel yielding failure mode.

The third step consisted of CLT connection tests. First, specimens made of non-perforated steel-plates, CLT pieces, and SDD were tested under quasi-static monotonic and reversed cyclic loads. These tests examined the over-strength of the dowels. Then, specimens of the same design, but with the IPSP used for connecting the individual CLT pieces were tested.

In the fourth step, the IPSP were used as hold-downs. Steel-plates with the same perforation geometry were welded on L-steel-profiles for connecting them to the foundation. Here, also quasi-static monotonic and reversed cyclic tests were performed.

## 2. Materials

Two different types of SDD were used: 1) Würth Bohrstabdübel [1], supplied by MTC Solutions; and 2) Pitzl SAF [2], supplied by Herrmann Timber Frames. In Table 1, the characteristic values and mechanical properties of the different SDD are given. The values in Table 1 refer to the smooth shank diameter and the length from head to tip of the dowel.

*Table 1: Characteristic values of Würth BSD [1], [3] and Heco SAF [2]*

Manufacturer	$L$ [mm]	$D$ [mm]	$M_{y,k}$ [Nm]	$N_{II}$ [N]	$N_{\perp}$ [N]
Würth	133	6.9	43.5	6,249	3,868
Heco	133	7.0	27.3	10,360	7,850

Steel-plates of grade 44W/300W according to [4] were selected. This grade is utilized in general fabrication and construction. For all performed tests the thickness of the steel-plates was 3/16", corresponding to 4.8mm and the outer dimensions were 100.0mm in width and 250.0mm in length. All steel-plates were supplied by Nechako Steel and Machine LTD, a metal processing company located in Prince George. In Table 2, the relevant mechanical properties are shown.

*Table 2: Mechanical properties of the steel-plates [4]*

$f_u$ [N/mm <sup>2</sup> ]	$f_y$ [N/mm <sup>2</sup> ]	$E$ [N/mm <sup>2</sup> ]
450	300	200.000

The wooden components of the test specimens consisted of 5-ply CLT panels fabricated by Structurlam Mass Timber Corporation. The CLT was produced according to ANSI/APA PRG 320 [5] and PR-L314 [6]. The fibre direction of the two outer plies and the middle ply (35mm thick) were orthogonal to the intermediate plies (17mm thick). The CLT with the trade name Crosslam was made of Spruce-Pine-Fire (SPF) wood with an average density of 485 kg/m<sup>3</sup> [7]. The average moisture content (MC) of CLT was measured as 13.6%. Three MC measurements were taken on each of the 38 specimens using a Delmhorst RDM3 electric resistance meter. By measuring the dimensions and weighing the CLT panels an average density of 486 kg/m<sup>3</sup> was determined.

### **3. Material Level Tests**

#### **3.1 Dowel Bending Tests**

To verify the mechanical properties of the dowels, three-point bending tests according to ASTM F1575 [8] were performed. The standard specifies a span of 11.5 times the dowel diameter. A displacement-controlled load rate of 6mm/min and a bearing length of 8mm between the supports were applied. For both types of SSD, eight replicates of bending tests were carried out using a 100kN MTS servo-hydraulic Test System. The bending test setup can be seen in Figure 2.

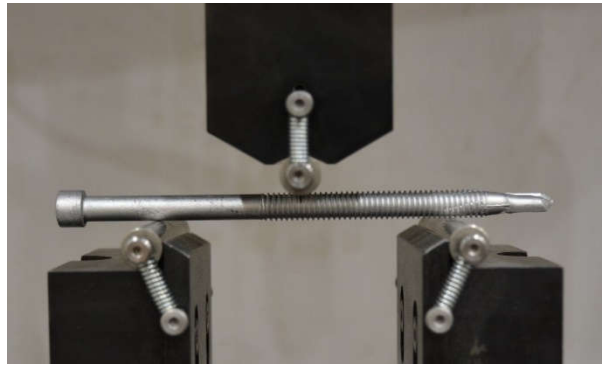


Figure 2: Dowel bending test setup

To determine the bending yield moment  $M_y$  of the SDD a straight line from the initial linear portion of the load-deformation curve is offset by 5% of the fastener diameter as shown in Figure 3. The load  $P$  that is required for calculating  $M_y$  (equation (1)) is the value where the offset line intersects the load-displacement curve.

$$M_y = P \times \frac{s_{bp}}{4} \tag{1}$$

$s_{bp}$  the span between the supports

This method was used to validate the values for the yield moment  $M_y$  given in Table 1.

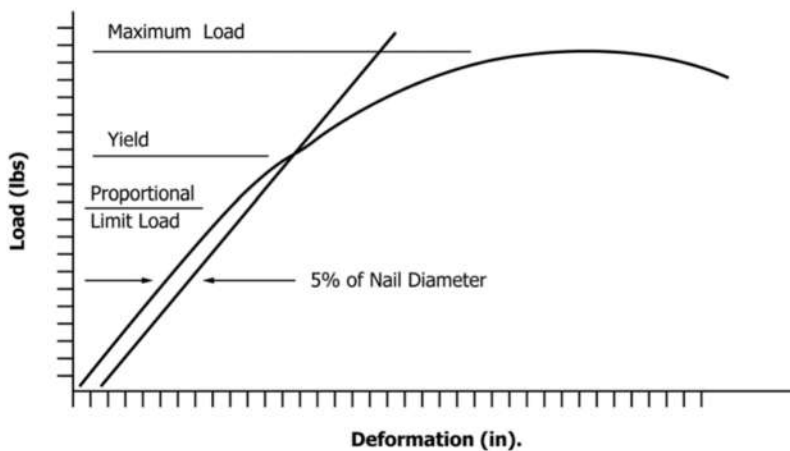


Figure 3: Load-deformation graph for dowel bending test [8]

### 3.2 Tension Tests of Neck-Shaped Steel-Plates

To validate the mechanical properties of the steel-plates, tension tests on neck-shaped steel-plates following ISO 6892-1:2016 [9] were conducted. The neck-shaped geometry (labelled Type-B) was necessary to avoid failure in the region of the attachments. In Figure 4, the steel-plates, as well as the tension test setup are shown. The specimens (five replicates) were clamped into the 100kN MTS Test System on both ends and subjected to a load rate of 3mm/min. The tests were stopped as soon as the steel reached the plastic range and only a minimal load increase could be detected with further deformation.

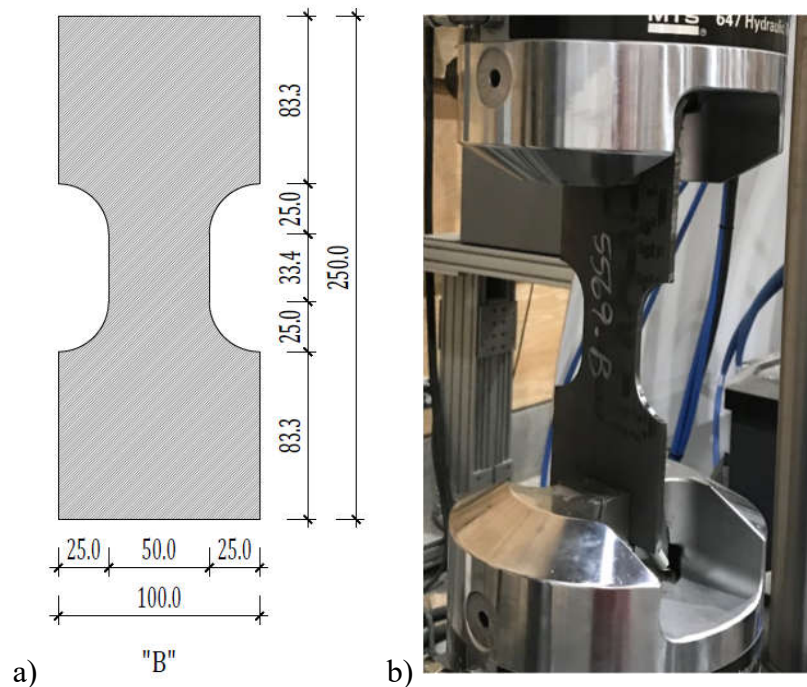


Figure 4: Type-B steel-plate: a) Geometry and b) tension test setup

### 3.3 Shear-Tension Tests of Perforated Steel-Plates

The performance of three different perforated steel-plate geometries (Figure 5) was investigated. The test series, labelled Type-C, Type-D, and Type-E differed in the number, width, and length of the steel “bridges”. The choice of the perforation geometry influences the ductility and the load-bearing capacity of the steel-plates. The steel-plates were clamped into the same testing machine as the Type-B steel-plates at an angle of about  $14.5^\circ$  (see Figure 6).

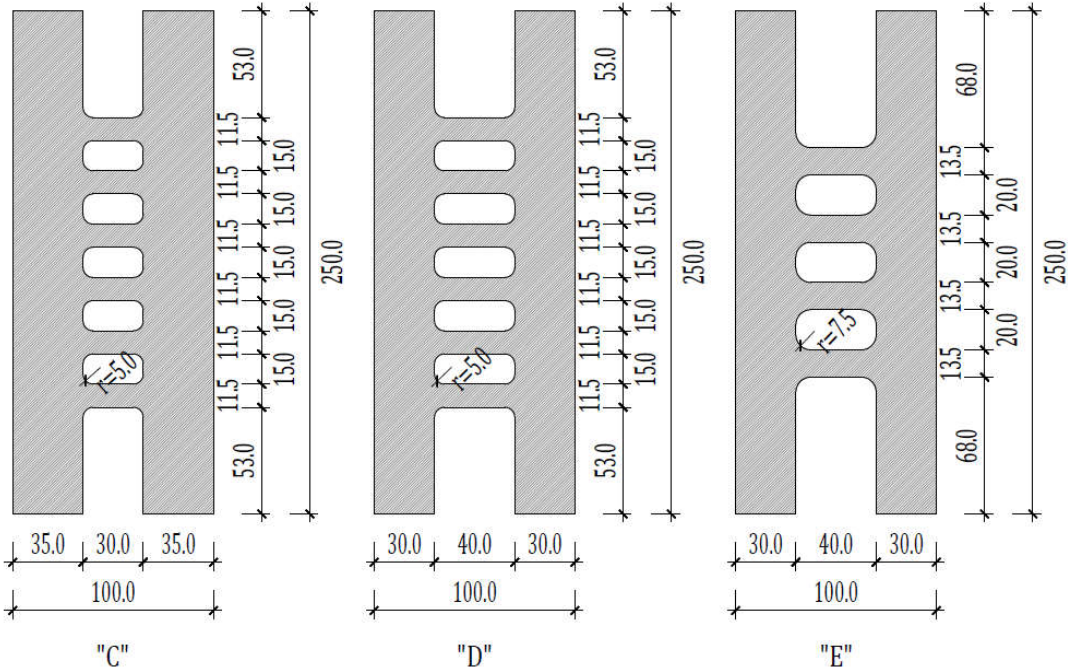


Figure 5: Geometries of steel-plates Type-C, Type-D, Type-E



Figure 6: Setup shear-tension test

## 4. Shear-Connection Tests

### 4.1 Overview

The tests on the connection level were divided into four series. For the first group, non-perforated steel-plates (labelled Type-A) were used to validate the SDD design values and their over-strength. The step was necessary to estimate the required number of SDD per shear plane in the specimens made with the IPSP so that all deformation and energy dissipation took place in the IPSP. For the other three test series, IPSP were applied with different plate geometries (Type-C, Type-D, or Type-E). Considering the results of shear-tension tests of the steel-plates, and the connection tests with non-perforated plates, the number of SDD was determined. Each specimen was specified by an individual identification label, with an example shown in Figure 7.

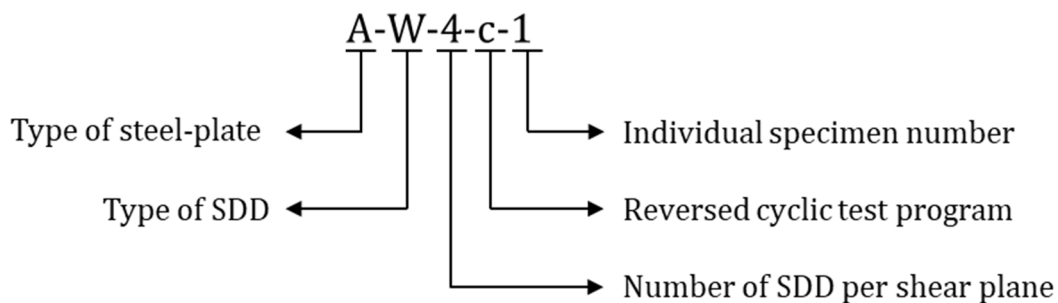


Figure 7: Explanation of the specimen's identification code

### 4.2 Specimen Geometry

Three 5-ply CLT pieces with a thickness of 139mm, a length of 300mm, and a width of 150mm for the outer pieces respectively 200mm for the inner piece were connected by one steel-plate per shear plane and a varying number of SDD, see Figure 8. To insert the steel-plates, 5mm wide and 50mm deep slots were cut into the middle of the narrow surfaces of the individual CLT pieces. It is recommended to pre-drill the steel and the wood with a ¼" diameter drill bit if the steel-plate is thicker than 3.2mm [3]. To meet the supplier's recommendations and facilitate the installation of the SDD, the 4.8mm thick steel-plates were pre-drilled, too. For the connection tests with the IPSP, specimens with the same geometry as the specimens with the non-perforated steel-plates were assembled. An example of a test specimen is shown in Figure 9.

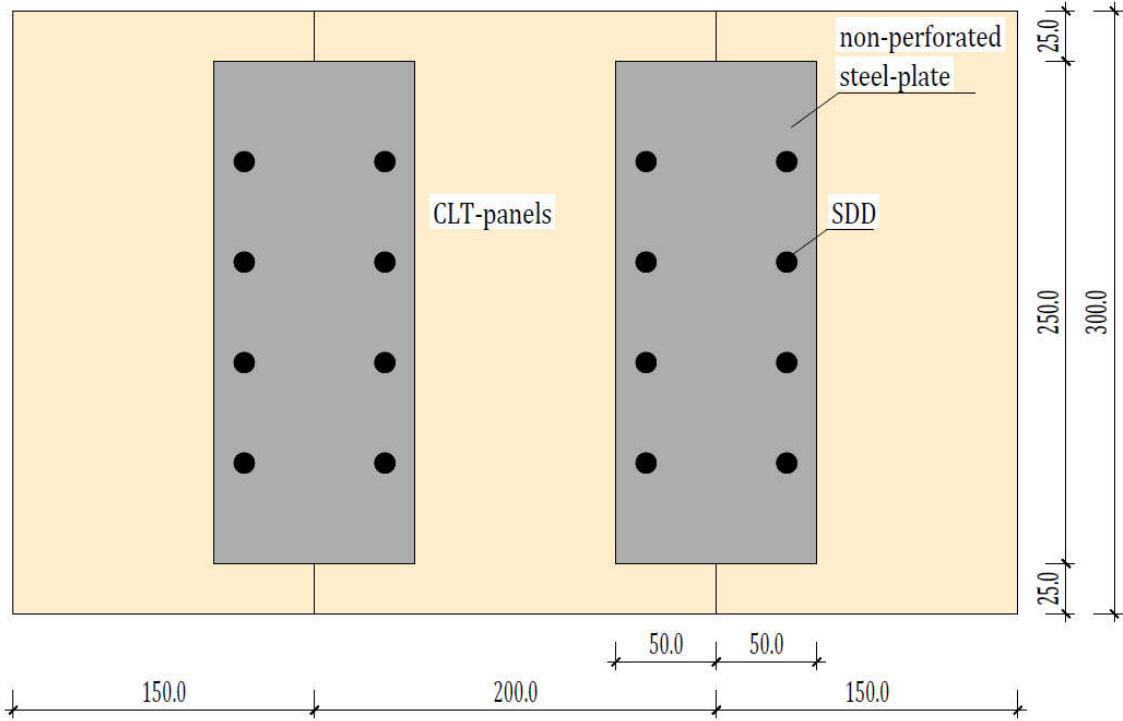


Figure 8: Specimen geometry with non-perforated steel-plates

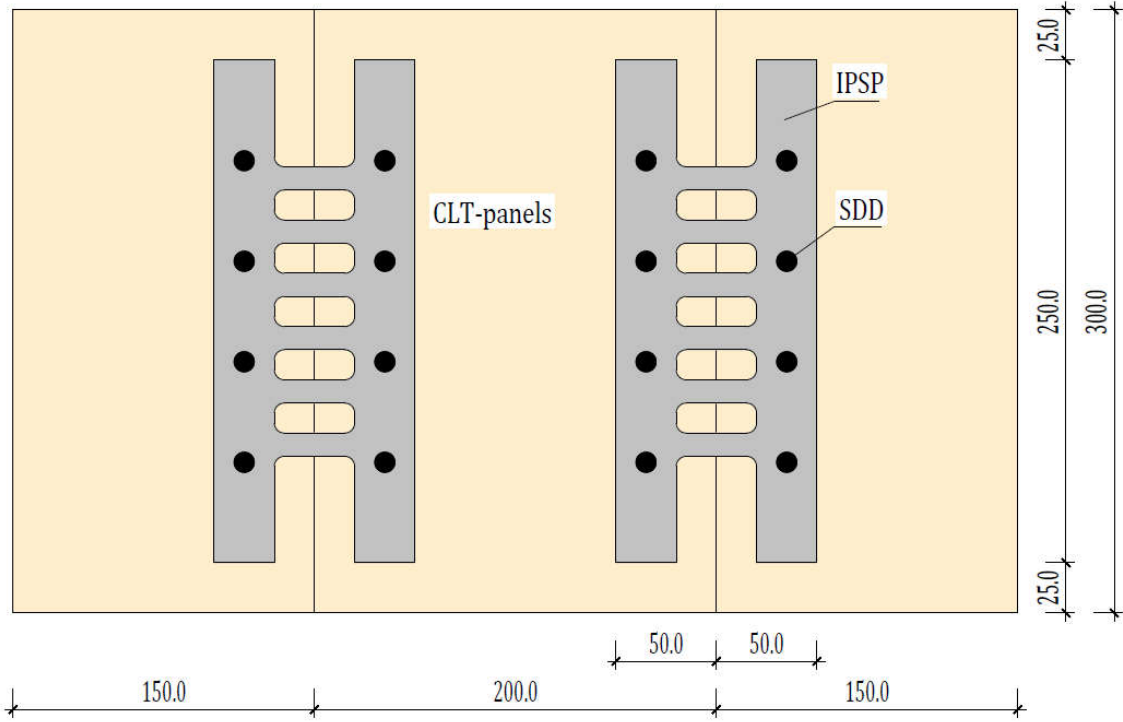


Figure 9: Specimen geometry with IPSP

### 4.3 Methods

For both, the quasi-static and the reversed cyclic tests a servo-mechanical universal test machine with a 250kN capacity was used. The two outer CLT parts were supported by wooden blocks and clamped down by a construction of threaded rods and square hollow steel profiles. Then the middle part of the specimen was loaded. The relative displacement between the outer and the middle part was measured by two Linear Variable Displacement Transducers (LVDT), see Figure 10.



*Figure 10: Test setup for quasi-static monotonic tests*

The quasi-static monotonic loading was applied according to EN 26891 [10]. First, the maximum load must be assumed. For the Type-A specimens, the values given by the SDD manufacturers were used. For the IPSP specimens, the results of the shear-tension tests were used to estimate the maximum load. The standard proposes to load the specimen with 40% of the estimated maximum load and to hold it for 30 seconds. Then the load was reduced to 10% and held for a further 30 seconds. In the last step of the test procedure, the load was increased until failure. If the actual measured maximum load and the estimated load differed more than 20%, the test program had to be adjusted. Failure was defined as the point at which the maximum load dropped by 20% of the maximum.

The resulting load-displacements were used for establishing the reversed cyclic loading protocol. The average displacement at the point of failure (80% of maximum load) must be taken. Then 60% of this displacement was used as the target displacement for the reversed cyclic tests. The test protocol for the reversed cyclic tests followed an abbreviated CURREE loading protocol [11]. The 100% value is divided into percentage steps that are run through with one cycle. Between each step, two cycles were run in which the deformation was reduced to 75% of the input value. The rate at which the test machine runs was staggered according to the same principle.

## **5. Hold-Down Tests**

### **5.1 Specimen Geometry**

In addition to the shear connection described in chapter 0, hold-downs are required to transfer the vertical uplift forces caused by lateral loads such as wind or earthquakes. The objective of the hold-down tests was to validate the performance of IPSP with SDD connections under a rocking kinematic motion.

The perforation geometry of the steel-plates used for the hold-downs was the same as in the shear-connection tests. Three different steel-plates (Type-C2, Type-D2, and Type-E2) were welded on L-steel-profiles (Figure 11). The 5-ply CLT panel had a dimension of 600mm in width and 1000mm in length. The results of the shear-connection tests were used to make an assumption about the performance and behaviour of the hold-down connection and estimate the number of required SDD. The preparation of the specimens followed the same steps as for the shear-connection tests described in chapter 0. To identify the specimens the same code as presented in chapter 0 was used.

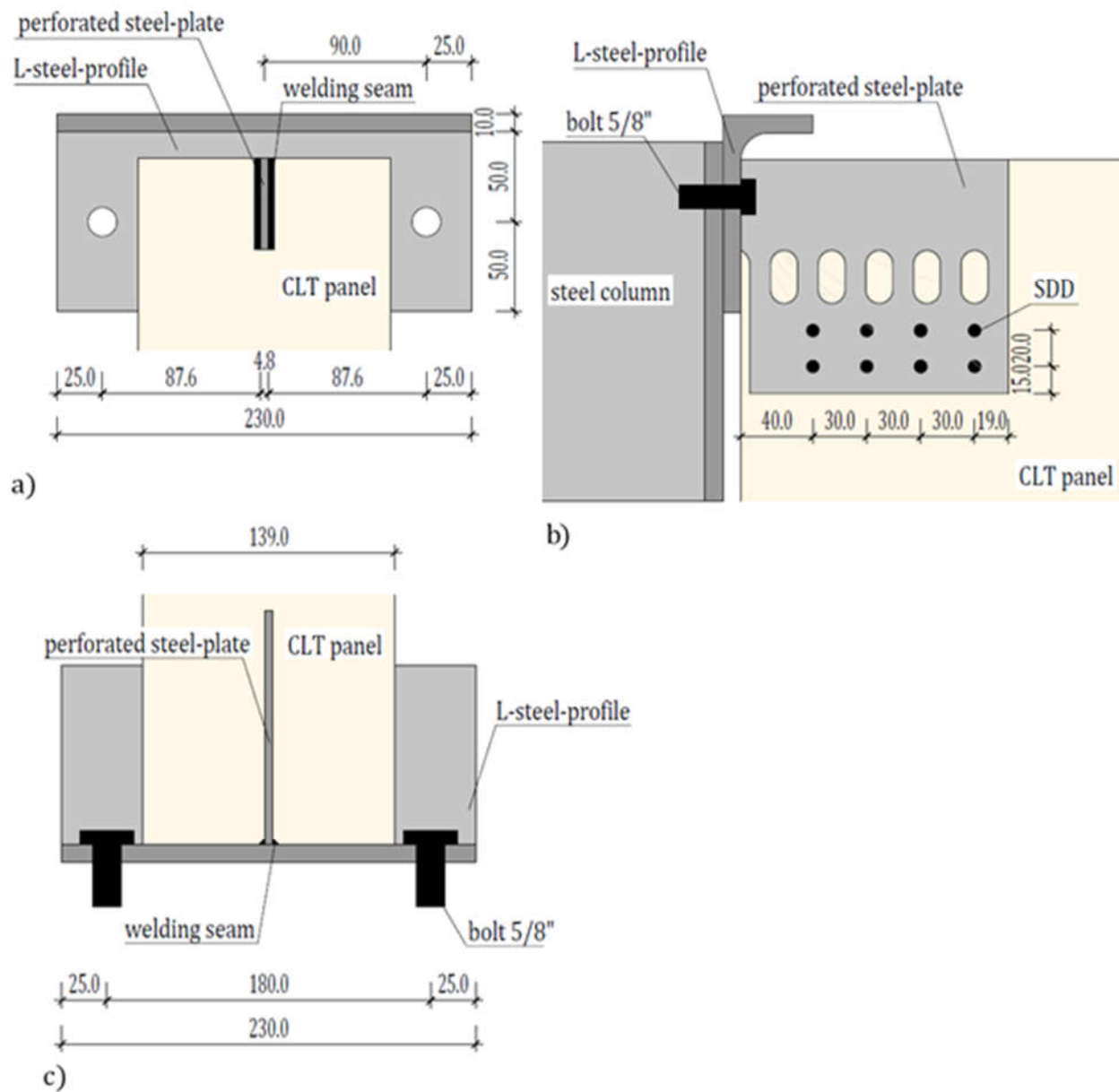


Figure 11: Geometry of hold-down: a) vertical section; b) side view; c) horizontal section

## 5.2 Methods

For the hold-down tests, the same servo-mechanical universal test machine as for the shear-connection tests was used. The specimen consisting of the CLT panel and the hold-down system was mounted to the steel column as shown in Figure 12. The pin connection at the bottom was realized by drilling a 1-9/16'' hole through the CLT panel and connect it to the test setup with a 1-1/2'' bolt. The load was applied 540mm from the corner of the CLT panel where the steel-plate was

mounted. The horizontal and vertical deflection was measured by two LVDTs (one LVDT on each side of the CLT panel) respectively. For the monotonic testing, the EN 26891 loading protocol [10] was used. The assumption of the maximum load was based on the results of the shear-connection tests. The procedure of the reversed cyclic test program was the same as for the shear-connection tests.

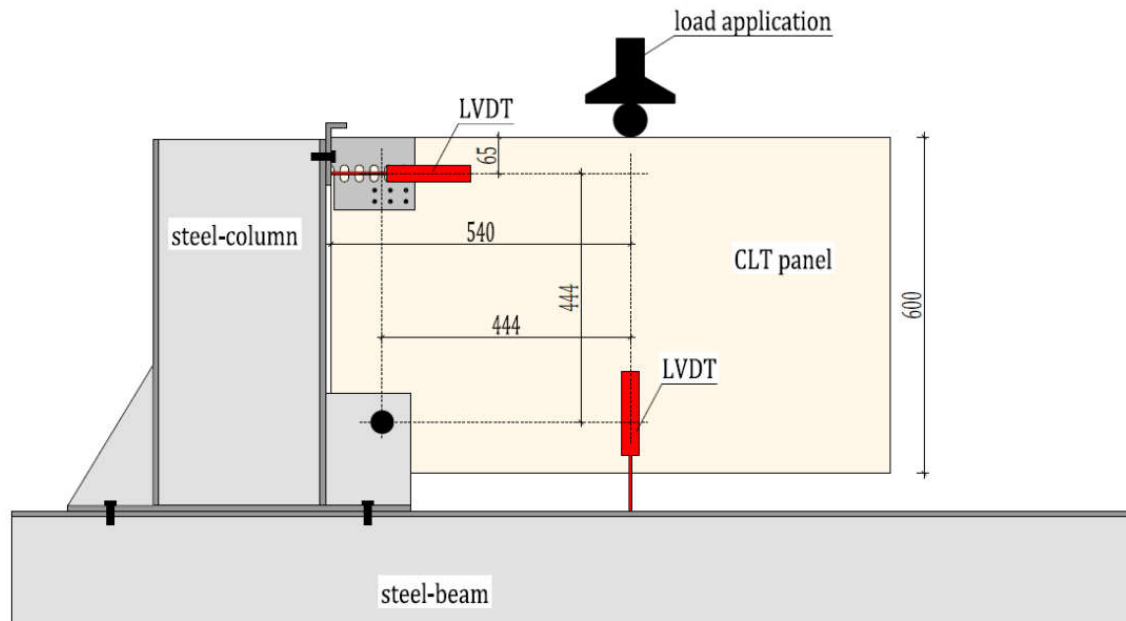


Figure 12: Hold-down test setup

## 6. Analysis

For both the quasi-static monotonic and reversed cyclic tests following characteristic values were obtained:

- maximum load,  $F_{max}$
- yield load,  $F_Y$
- displacement at maximum load,  $d_{F_{max}}$
- displacement at yield load,  $d_{F_Y}$
- stiffness,  $k$
- ductility,  $\mu$

Stiffness was calculated in accordance with EN-26891 [10] for the range of the load-displacement curves between 10% and 40% of the maximum load. The ductility  $\mu$  is calculated taking the ratio

between the ultimate displacement  $d_{ult}$  and the displacement at yield load  $d_{F,y}$  with the scale as proposed by Smith et al. [12] being used: brittle ( $\mu \leq 2$ ), low ductility ( $2 \leq \mu \leq 4$ ), moderate ductility ( $4 \leq \mu \leq 6$ ) and high ductility ( $\mu > 6$ ).

In general, the average between the two LVDTs was used for the displacements shown in the tables. For every test series, in addition to the individual results, the average of the recorded parameters and the coefficient of variation (COV) was computed. The COV is the ratio of the standard deviation to the average, it is a measure of relative variability [13].

To calculate load and displacement at yield, equivalent energy elastic-plastic (EEEEP) curves according to ASTM 2126-19 [14] were developed for each specimen, see Figure 13. The first step was to create the envelope curves by connecting the load peaks and their related displacements for each cycle. Then, interpolated curves were developed. On the basis of the envelope curves, by applying several interpolations, more data points were calculated to get more exact values for the yield loads and corresponding displacements. Finally, EEEP curves were developed based on the interpolated curves.

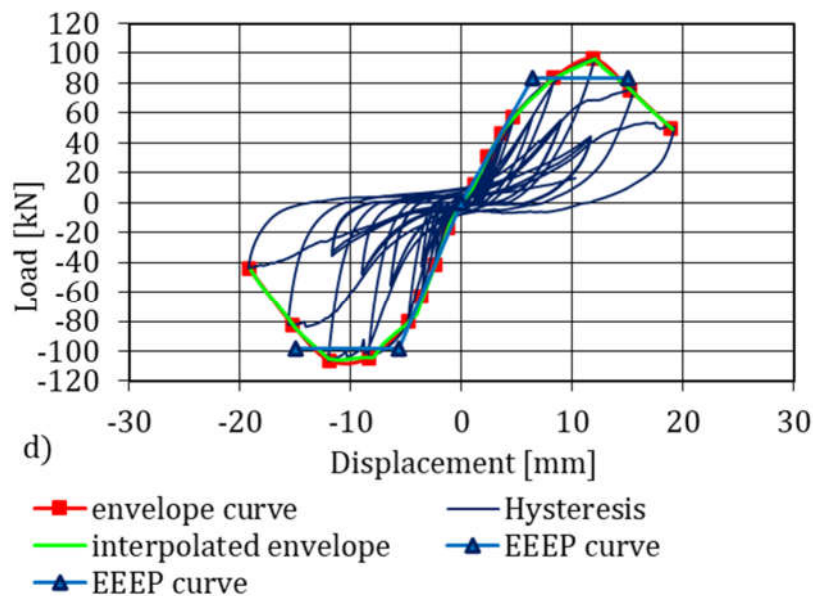


Figure 13: Development of EEEP curves: a) Envelope curve, b) Interpolated curve, c) EEEP curve, d) Combined curves

## 7. Results

### 7.1 Dowel Bending Tests

The results from the dowel bending tests are summarized in Table 3. A representative sample of each type of SDD is shown Figure 15).

Table 3: SSD bending test results

	$F_{max}$	5% Offset		$F_{max}$	5% Offset
SAF	[kN]	[kN]	BSD	[kN]	[kN]
Average	3.4	2.7	Average	3.0	2.4
COV	2%	2%	COV	4%	4%

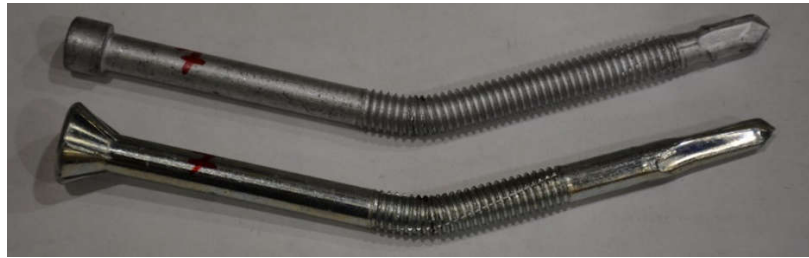


Figure 14: SDD bending failure

Applying equation (1) following yield moments were calculated:

$$\text{Heco SAF: } M_y = 2,700N \times \frac{0,08m}{4} = 54Nm$$

$$\text{Würth BSD: } M_y = 2,400N \times \frac{0,08m}{4} = 48Nm$$

The load-displacements are illustrated in Figure 15. First, the SDD maintained a linear load-deformation response. Then, the gradient of the straight line became less until a significant deformation occurred while maintaining the ultimate load. Following the fracture on the tension face of the fastener, an abrupt loss of load occurred. The biggest difference in the load-displacement curves can be seen in the amount of displacement before the load dropped abruptly and the dowels failed. Otherwise, the load-displacement responses for both types of SDD provided very consistent results and the ultimate loads for all tests provided relatively low COVs of 2% (HECO SAF) and 4% (Würth BSD).

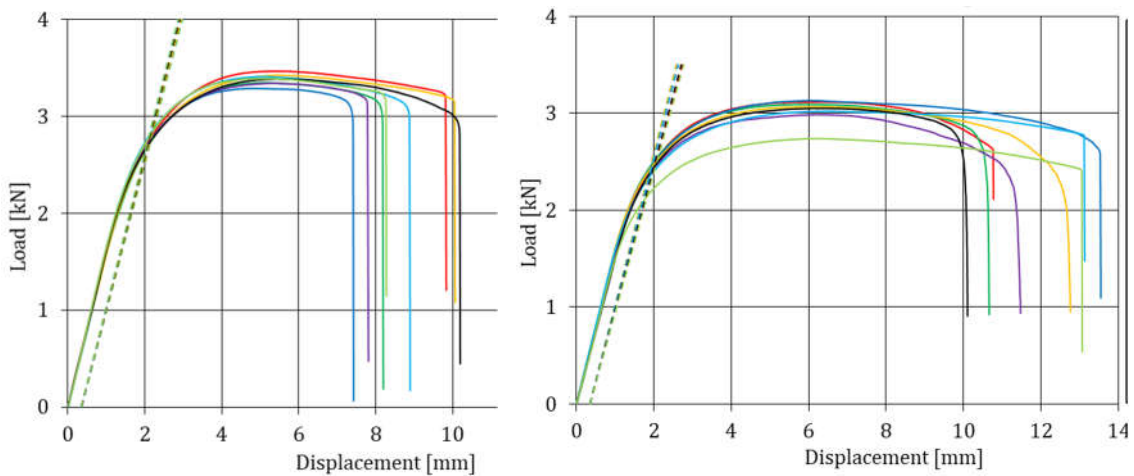


Figure 15: Bending tests load-displacement, a) Heco SAF; b) Würth BSD

## 7.2 Steel-Plate Tests

The results from the Type-B tension tests are summarized in Table 4, Figure 16 shows the three different steel-plate geometries tested in the shear-tension. The solid steel portions on the left and right sides of the perforations were moved parallel against each other, and the load-displacement curves are illustrated in Figure 17. The load-displacement graphs showed a linear behaviour accompanied by small displacements until the yield load was reached. Then the load dropped a bit before it increased again accompanied by large deformations. The most important result from the shear-tension tests was the yield load  $F_Y$ . The approximate values for  $F_Y$  for the different steel-plate geometries are listed in Table 5.

Table 4: Type-B tension test results

Test	$F_{max}$ [kN]	$d_{F_{max}}$ [mm]	$F_Y$ [kN]	$d_{F_Y}$ [mm]
Average	97.1	6.2	81.4	1.1
COV	2%	10%	1%	6%

Table 5: Yield loads from shear-tension tests

Type	$F_Y$ [kN]
Type-C	32
Type-D	22
Type-E	22

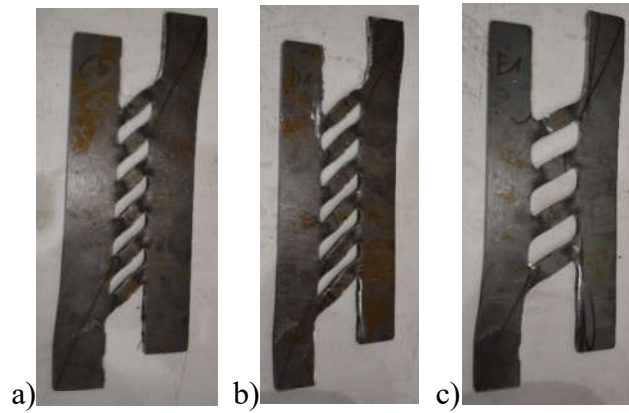


Figure 16: Tested steel-plates: a) Type-C; b) Type-D; c) Type-E

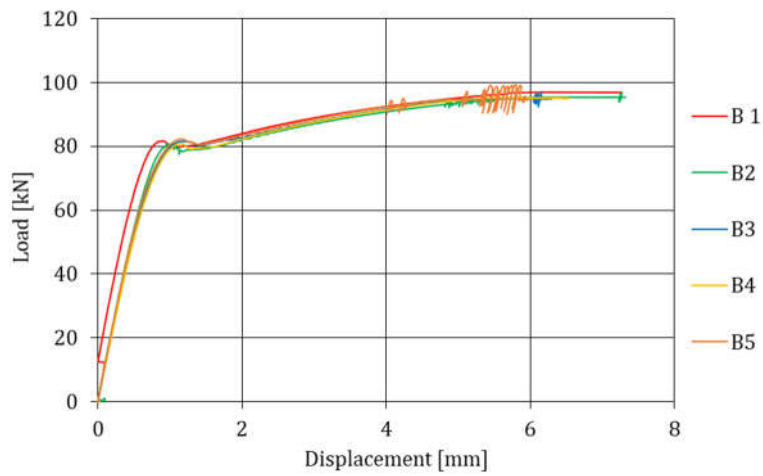


Figure 17: Type-B tension tests load-displacement

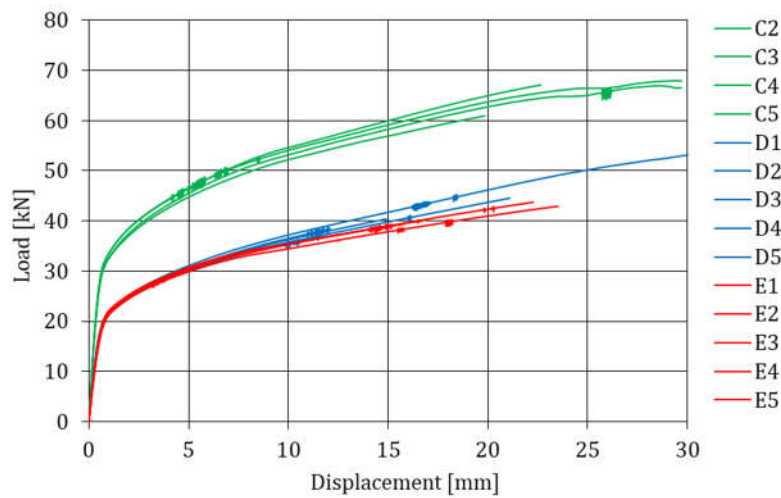


Figure 18: Type-C, Type-D, Type-E shear-tension test load-displacement

### 7.3 CLT Shear-Connection Tests

The average results and COVs from the Type-A shear-connection tests are summarized in Table 6 and the load-displacement curves are illustrated in Figure 19 and Figure 21.

Table 6: Results summary Type-A shear-connection tests

Series	Repl.		$F_{max}$ [kN]	$F_Y$ [kN]	$d_{Fmax}$ [mm]	$d_{FY}$ [mm]	$k$ [kN/mm]	$\mu$ [-]
A-W-2-m	4	Average	61.7	55.1	12.4	2.3	20.1	7.6
		COV	9%	9%	25%	28%	17%	20%
A-W-2-c	4	Average	55.0	49.9	13.1	6.3	8.9	3.2
		COV	3%	2%	4%	41%	27%	28%
A-W-4-m	4	Average	116.6	105.8	17.3	2.3	37.3	12.0
		COV	1%	1%	8%	16%	16%	33%
A-W-4-c	5	Average	105.6	95.0	13.7	5.6	18.0	3.4
		COV	4%	3%	3%	5%	5%	6%
A-H-4-m	2	Average	110.8	99.1	9.2	2.0	44.4	13.4
		COV	0%	2%	13%	46%	32%	55%
A-H-4-c	5	Average	98.1	85.5	11.8	6.4	13.7	2.6
		COV	4%	4%	2%	15%	18%	11%

For the monotonic tests, the general load-displacement behaviours were the same for all specimens. First, the response was linear until the point of 40% of the estimated maximum load was reached and the load dropped to 10 % of the estimated maximum load. After this point, the loads increased non-linearly until the wood and the SDD started to fail. These failure mechanisms were characterized by the irregular jagged course of the graphs (see Figure 19). In Figure 20 the tested specimens with the Type-A steel-plates and the different types and number of SDD are shown. In all three test series, the CLT panel in the middle was moved against the outer two panels and on the bottom of the specimen a horizontal deflection could be observed. Due to the bending of the SDD, the dowel heads were pushed into the wood.

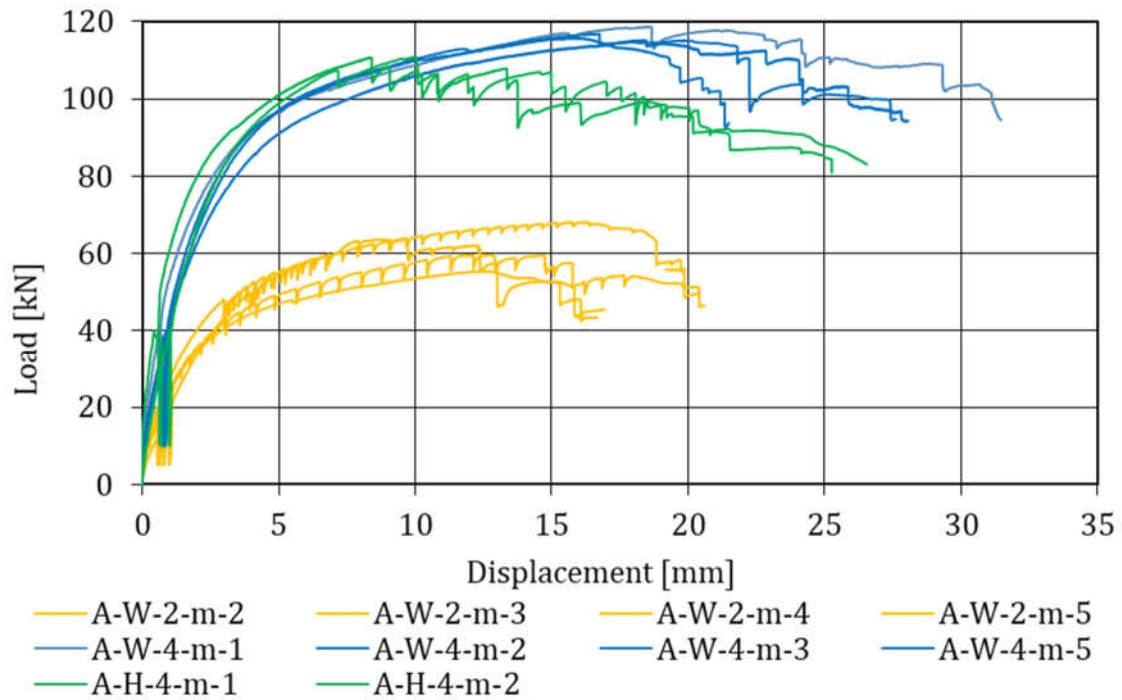


Figure 19: Type-A monotonic tests load-displacement

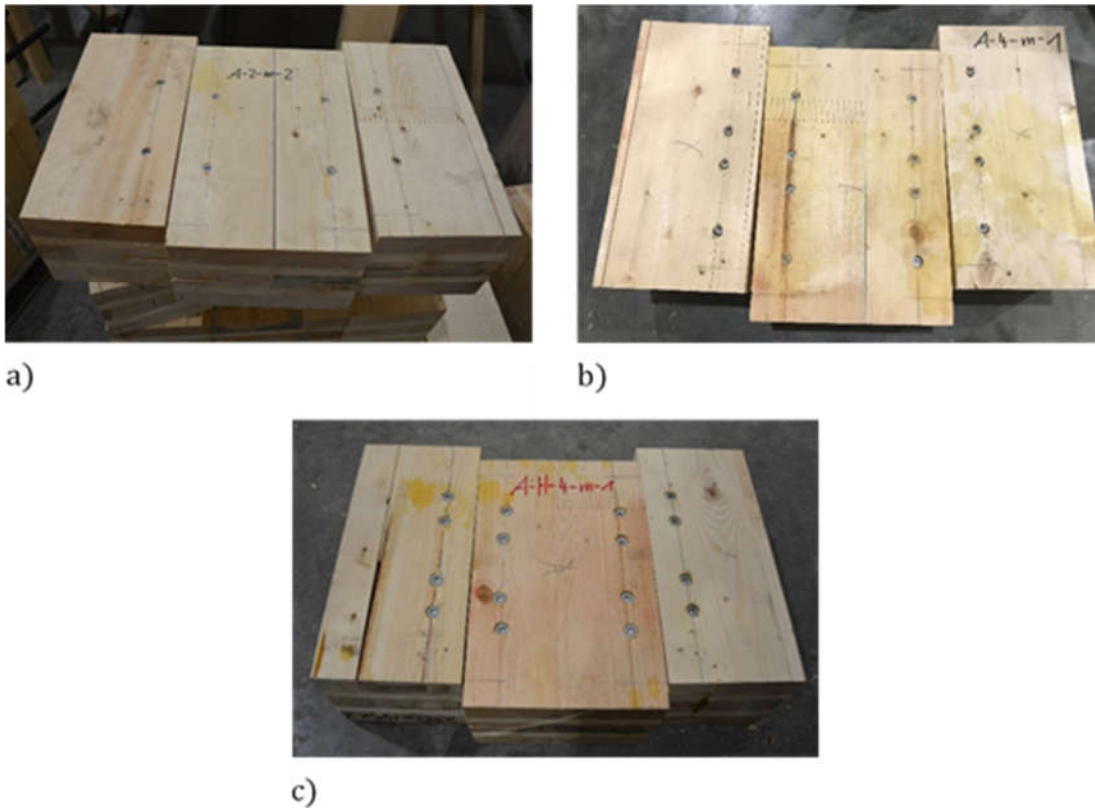


Figure 20: Tested specimens: a) A-W-2-m; b) A-W-4-m; c) A-H-4-m

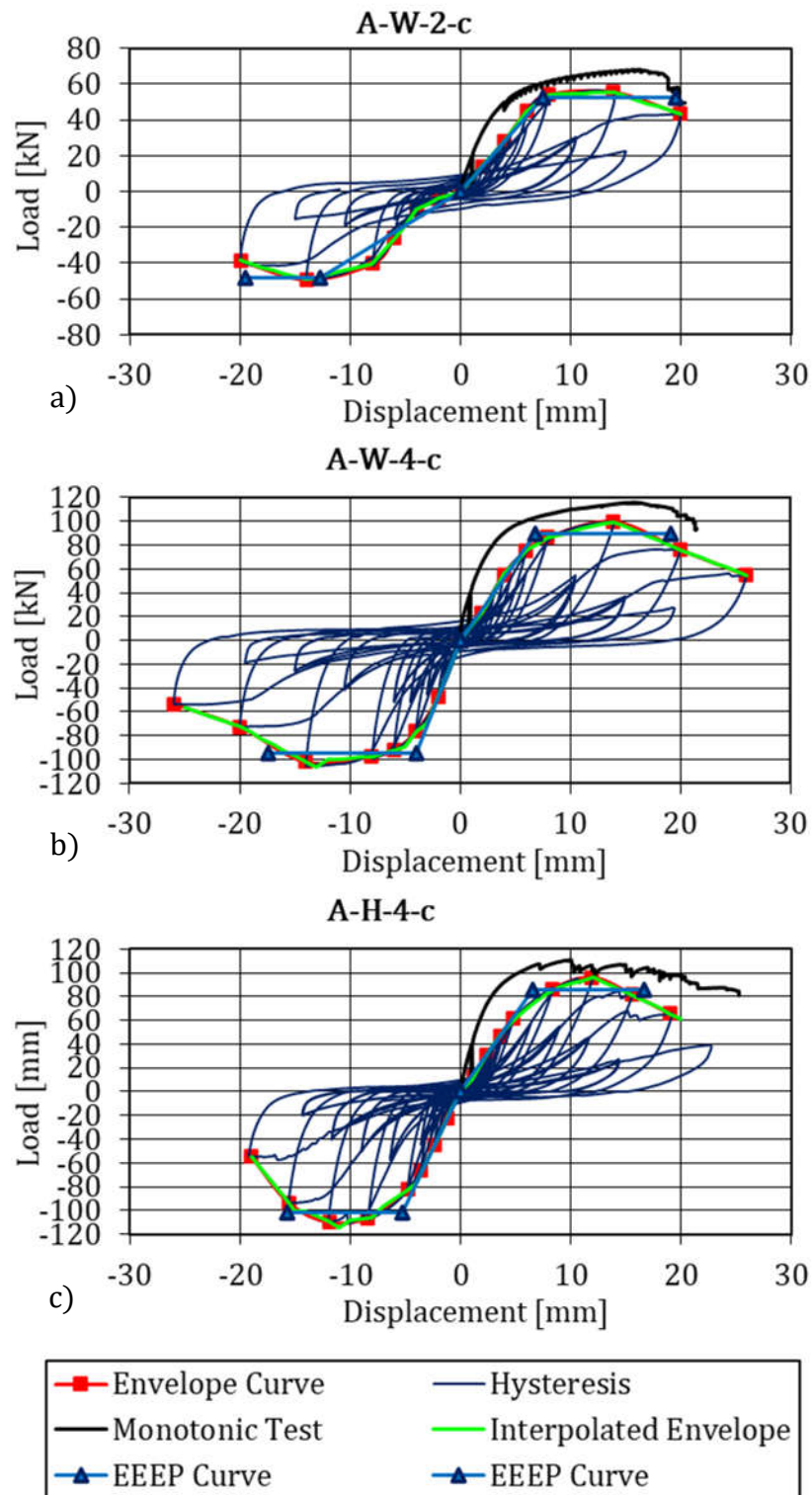


Figure 21: Typical load-displacement: a) A-W-2-c; b) A-W-4-c; c) A-H-4-c

The average results and COVs from the monotonic and cyclic shear-connection tests of the Type-C, Type-D, and Type-E specimens are summarized in Table 7 and the load-displacement curves are illustrated in Figure 22 and Figure 25.

Table 7: Results summary Type-C, Type-D, Type-E shear-connection tests

Series	Repl.		$F_{max}$ [kN]	$F_Y$ [kN]	$d_{Fmax}$ [mm]	$d_{FY}$ [mm]	$k$ [kN/mm]	$\mu$ [-]
C-H-6-m	2	Average	155.4	129.0	27.3	2.4	44.7	15.3
		COV	4%	7%	14%	16%	5%	18%
C-H-6-c	5	Average	116.3	102.9	15.1	6.1	17.0	3.0
		COV	3%	3%	11%	6%	5%	5%
D-H-6-m	2	Average	151.6	122.0	27.5	4.3	25.6	11.3
		COV	1%	1%	10%	46%	43%	22%
D-H-6-c	5	Average	94.4	78.6	17.4	5.2	15.2	3.7
		COV	2%	2%	0%	5%	5%	4%
E-W-4-m	2	Average	109.6	92.9	31.1	2.7	30.5	17.1
		COV	3%	2%	32%	26%	21%	18%
E-W-4-c	5	Average	87.7	75.1	17.4	5.8	13.2	3.4
		COV	4%	2%	0%	4%	4%	6%

For each monotonic test series, two replicates were tested. The course of the graphs was created in the same way as for the Type-A monotonic tests. Compared to the Type-A specimens, the parallel movement of the outer and inner CLT panels against each other was much greater. Due to bending effects, some of the dowel heads were pushed into the CLT (see Figure 23).

For the load-displacement curves of the cyclic tests, one typical curve is given for each test series in Figure 25. The cyclic test specimens with the IPSP did not fail abruptly, but constantly lost capacity with every further cycle above a certain maximum load. After the tests, all three different types of specimens were usually divided into three single parts (see Figure 24a) and the steel “bridges” were ruptured (see Figure 24b) The SDD were not or only slightly bent and could be used again.

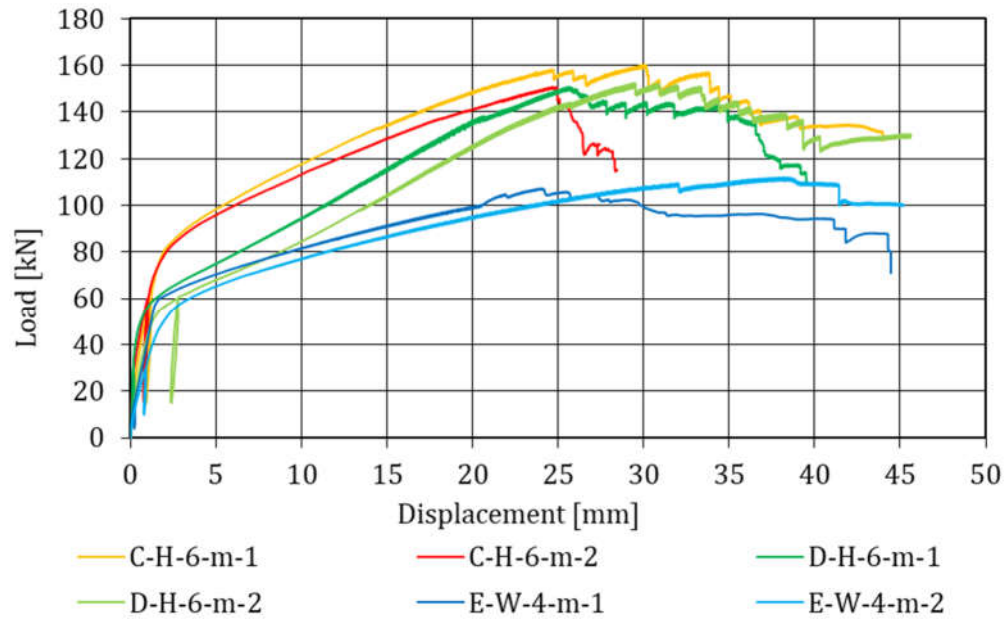


Figure 22: Type-C, Type-D, Type-E shear-connection monotonic load-displacement



Figure 23: Typical test specimen for monotonic IPSP shear-connection tests



Figure 24: a) Typical test specimen for cyclic IPSP shear connection tests; b) ruptured steel bridges

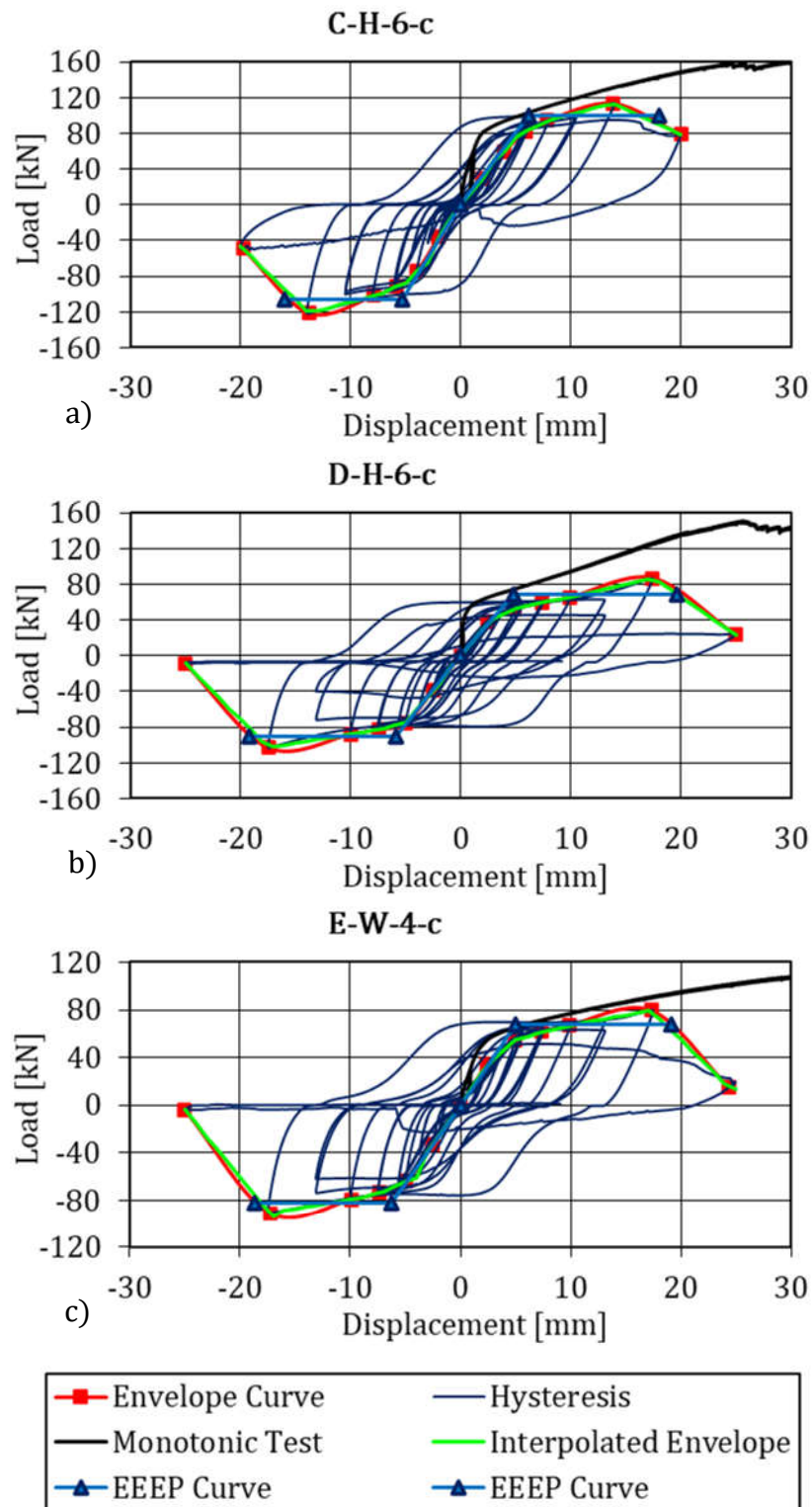


Figure 25: Typical cyclic load-displacement: a) Type-C; b) Type-D, and c) Type-E

#### 7.4 Hold-Down Tests

The average results and COVs from the monotonic and cyclic hold-down tests are summarized in Table 8, and the load-displacement curves are illustrated in Figure 26 and Figure 28.

Table 8: Results summary Type-C2, Type-D2, Type-E2 hold-down tests

Series	Repl.		$F_{max}$ [kN]	$F_Y$ [kN]	$d_{Fmax}$ [mm]	$d_{FY}$ [mm]	$k$ [kN/mm]	$\mu$ [-]
C2-H-m	2	Average	57.8	51.6	20.7	4.1	10.3	7.8
		COV	2%	1%	25%	15%	21%	19%
C2-H-c	3	Average	92.5	84.2	33.7	21.5	3.9	2.3
		COV	14%	13%	9%	11%	13%	7%
D2-H-m	3	Average	61.7	51.7	27.7	5.8	6.8	7.5
		COV	10%	9%	8%	18%	12%	19%
D2-H-c	3	Average	79.6	66.8	31.9	19.2	3.5	1.9
		COV	3%	6%	0%	4%	4%	9%
E2-H-m	3	Average	45.7	39.5	27.7	5.4	5.8	6.1
		COV	8%	7%	24%	25%	24%	19%
E2-H-c	3	Average	68.0	57.4	30.7	12.5	4.8	3.0
		COV	10%	6%	5%	24%	24%	25%

The observed load-displacement behaviour of the monotonic tests in the hold-down tests was similar to the shear-connection tests. The response of the specimens was linear until 40% of the assumed maximum load was reached. In the second load cycle, the curves showed a homogenous growth until the steel-plates and the SDD started to fail (irregular jagged part of the curves). The Type-C2 steel-plate geometry was not deformed much, but the SDD were pushed into the wood due to bending of them (Figure 27a), while the Type-D2 and Type-E2 geometries were deformed very strong until some of the steel “bridges” broke (Figure 27b), but the SDD were not deformed significantly. In Figure 28 one typical load-displacement curve for each cyclic hold-down test series is illustrated. The cycles of the cyclic hold-down tests started at a certain zero position and only went in positive direction which described the most significant difference to the cyclic testing of the shear-connection specimens.

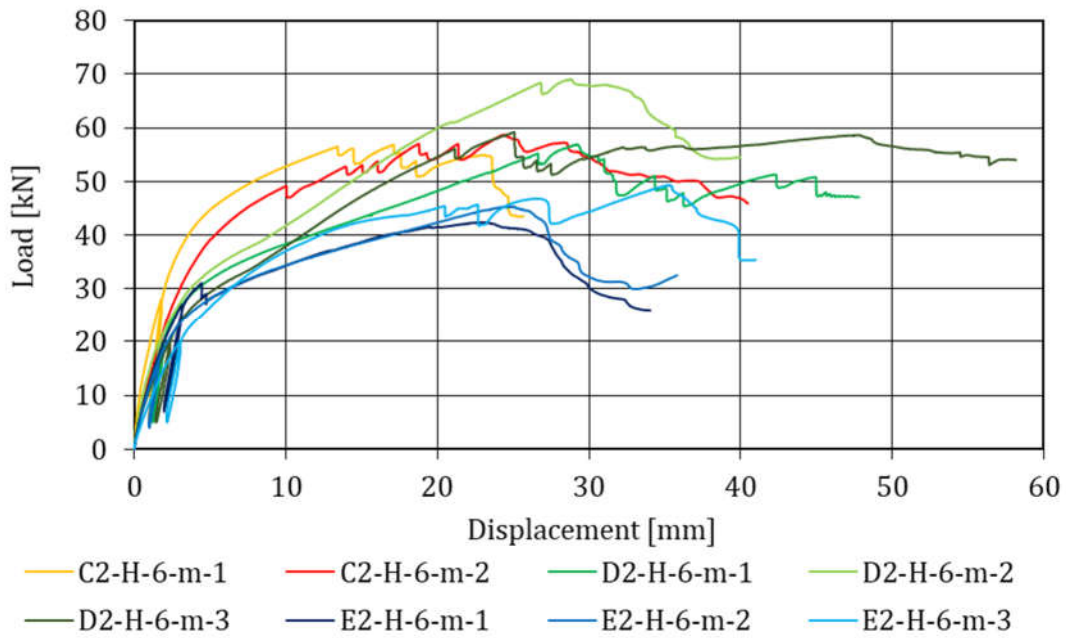


Figure 26: Type-C2, Type-D2, Type-E2 monotonic hold-down tests load-displacement

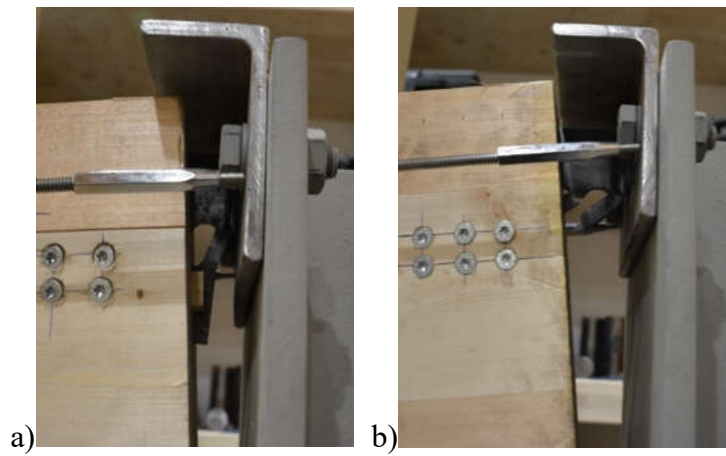


Figure 27: Monotonic hold-down tests: a) Type-C2; b) Type-E2

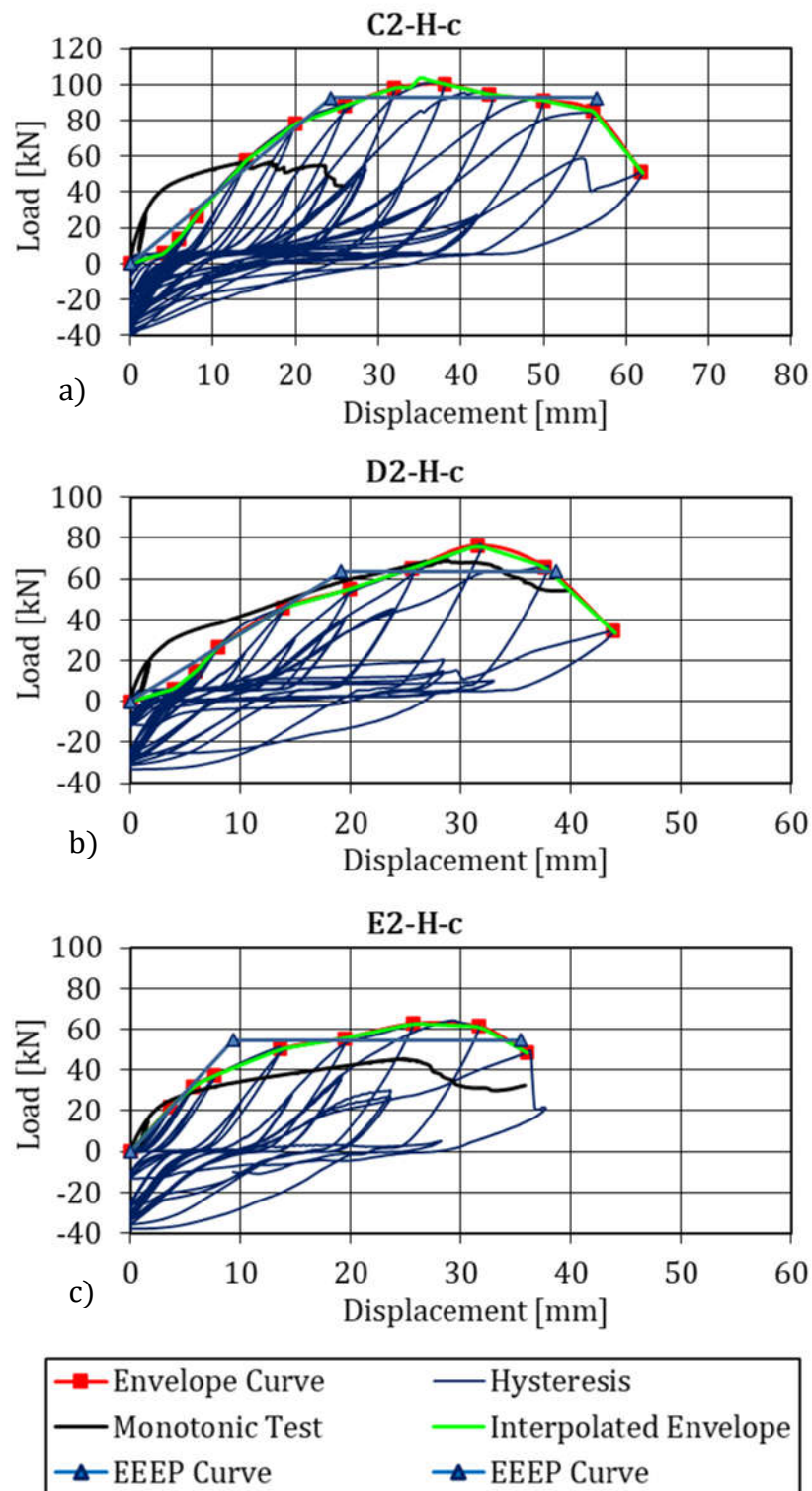


Figure 28: Typical cyclic hold-down load-displacement: a) Type-C2, b) Type-D2, and c) Type-E2

## References

- [1] American National Standard Institute, „ANSI/APC PRG 320: Standard for Performance-Rated Cross-Laminated Timber,“ ANSI, New York, 2019.
- [2] MTC Solutions, „Self-Drilling Dowels Design Guide,“ [Online]. Available: <https://mtcsolutions.com/resource/self-drilling-dowel-design-guide/>. [Zugriff am 11 05 2020].
- [3] ASTM International, „F1575-17; Standard Test Method for Determining Bending Yield Moment of Nails,“ West Conshohocken, 2017.
- [4] Würth, „Leistungserklärung Nr. LE\_ 5394216073\_00\_M\_Bohrstabdübel BSD,“ Künzelsau, 2015.
- [5] EFG, Heco Italia, „Dichiarazione di Prestazione Nr. DoP EFG 001-14,“ Romano d’Ezzelino, 2014.
- [6] Canadian Standards Association, „CSA-S16-01,“ CSA, 2007.
- [7] APA - The Engineered Wood Association, „APA PR-L314,“ APA, Tacoma, Washington, 2020.
- [8] Structurlam Mass Timber Corporation, „Crosslam CLT Technical Design Guide v4.0,“ Penticton, BC.
- [9] International Organisation for Standardization, „ISO 6892-1:2016 Metallic materials - Tensile testing - Method of test at room temperature,“ ISO, 2016.
- [10] European Committee for Standardization, „EN 26891 Timber structures; Joints made with mechanical fasteners; General principles for the determination of strength and deformation characteristics,“ CEN, Belgium, 1991.
- [11] I. Smith, A. Asiz, M. Snow und Y. Chui, „Possible Canadian/ISO Approach to Deriving Design Values From Test Data,“ in *Proceedings of CIB-W18 Timber Structures, Meeting 39 (Paper 39-17-1)*, Florence, Italy., August 28-31, 2006,.
- [10] ASTM International, „E2126-19: Standard Test Methods for Cyclic (Reversed) Load Test for Shear Resistance of Vertical Elements of the Lateral Force Resisting Systems for Buildings,“ West Conshohocken, 2019.

## **Acknowledgments**

This project was funded by British Columbia Forest Innovations Investment through a Wood First Grant to the University of Northern British Columbia (UNBC).

Following companies supported the project application and/or the actual project:

- Aspect Structural Engineers
- Fast+Epp
- FPInnovations
- MTC Solutions
- Structurlam Mass Timber Corporation
- Hermann Timber Frames

The material used for the research was partially donated and partially provided at reduced cost by MTC Solutions, Structurlam Mass Timber Corporation and Hermann Timber Frames.

The support provided by the UNBC's lab technicians Michael Billups and Ryan Stern is greatly appreciated.